J Appl Electrochem (2012) 42:69–74
DOI 10.1007/s10800-011-0372-2

ORIGINAL PAPER

Preparation and electrochemical properties of SiO_2–non-graphitizable carbon composites as negative electrode materials for Li-ion batteries

Takayuki Doi · Masao Tagashira · Yasutoshi Iriyama · Takeshi Abe · Zempachi Ogumi

Received: 20 November 2008 / Accepted: 13 April 2009 / Published online: 17 December 2011

Abstract SiO_2–non-graphitizable carbon composites were prepared by pyrolysis of a mixture of ethyl cellulose and nano-sized SiO_2. The composite electrode showed high reversibility in insertion and/or extraction reactions of Li ions at potentials below 1 V with little hysteresis after the 2nd cycle, whereas a large irreversible capacity was observed in the 1st cycle. This reversible capacity increased with increasing SiO_2 content above 5 wt%. Li ion transfer at the interface between a composite electrode and an electrolyte was studied by ac impedance spectroscopy. In the Nyquist plots, a semi-circle that was assigned to charge-transfer resistance (R_{ct}) because of Li ion transfer across the interface between the composite electrode and electrolyte appeared at potentials below 1 V. The values of R_{ct} decreased with increasing SiO_2 content. These results indicate that both a decrease in R_{ct} and an increase in reversible capacity can be achieved by use of SiO_2–non-graphitizable carbon composite electrodes; this would lead to Li-ion batteries with higher power and energy density.

T. Doi
Institute for Materials Chemistry and Engineering,
Kyushu University, 6-1 Kasuga-koen, Kasuga 816-8580, Japan

Present Address:
T. Doi (✉)
Office of Society-Academia Collaboration for Innovation,
Kyoto University, Gokasho, Uji 611-0011, Japan
e-mail: doi@saci.kyoto-u.ac.jp

M. Tagashira · T. Abe · Z. Ogumi
Graduate School of Engineering, Kyoto University,
Nishikyo-ku, Kyoto 615-8510, Japan

Y. Iriyama
Department of Materials Science & Chemical Engineering,
Faculty of Engineering, Shizuoka University, 3-5-1 Johoku,
Hamamatsu 432-8561, Japan

Keywords Non-graphitizable carbon · Silicon oxide · Negative electrode · Lithium-ion battery

1 Introduction

Li-ion batteries are now used in a wide variety of portable electronic devices. Because of their high energy density, Li-ion batteries have been considered as possible power sources for hybrid electric vehicles (HEV). However, before Li-ion batteries can be used in high-power applications, their energy density and rate capability performance must still be improved. Different kinds of carbonaceous material have been studied for use as the negative electrode in Li-ion batteries [1]. Natural graphite and highly graphitized carbonaceous materials, which have acceptably high capacity and a very flat potential close to that of Li metal in charge–discharge processes, have been generally used for commercial Li-ion batteries [2]. However, other carbonaceous materials must be studied to enhance the performance of Li-ion batteries. Among these, a non-graphitizable carbon electrode gives a relatively high capacity in a wide potential range between 0 and 1 V, which makes it easy to monitor the residual battery capacity in terms of the battery voltage. Furthermore, because non-graphitizable carbon works at high operating potentials compared with graphite, the reductive decomposition of electrolytes can be suppressed. Hence, non-graphitizable carbon is a possible candidate for use as the negative electrode in Li-ion batteries in HEV.

Rapid charge and discharge reactions are required if Li-ion batteries are to be used for high-power applications. Rapid interfacial Li ion transfer and rapid Li ion transport through the electrodes and electrolyte is essential for improving the rate performance of Li-ion batteries. Non-graphitizable carbon, in contrast with graphite which has a

layered structure with perfect stacking order of graphene sheets, is composed of heavily interlaced or intertwined stacks of graphite-like layers. Because of this isotropic structure, non-graphitizable carbon has a relatively large number of Li ion insertion sites on the electrode surface. Therefore, charge-transfer resistance is expected to be small, and non-graphitizable carbon may be suitable for rapid interfacial Li ion transfer.

We previously studied Li ion transfer kinetics at a non-graphitizable carbon electrode–electrolyte interface by ac impedance spectroscopy [3, 4]. In that study, high activation barriers at the interface between the electrode and electrolyte for Li ion transfer were noted. On the other hand, our group previously prepared a $LiCoO_2$ film surface-modified with MgO and studied the effects of surface modification on Li ion transfer at an electrode–electrolyte interface [5]. These results showed that the activation energy for interfacial Li ion transfer could be reduced by surface modification with ceramic oxides. Sawai and Ohzuku [6] suggested that the limited transport of Li ions within an electrolyte in an electrode mix layer could be responsible for the rate performance of the batteries. Hence, Li ion conductivity of the electrolyte contained in the electrode mix layer should be enhanced for high-power batteries.

Mizuhata et al. [7] studied Li ion kinetics in an electrolyte solution of EC containing 1.0 mol dm^{-3} $LiClO_4$ and SiO_2 particles, and reported that the activation energy for Li ion conductivity decreased with addition of ceramic particles such as SiO_2. In addition, Croce et al. [8] studied the Li ion conductivity of composite electrolytes based on polyethylene oxide containing Li salts, for example $LiClO_4$ or $LiN(CF_3SO_2)_2$, and ceramic particles, for example SiO_2 and Al_2O_3. These results suggested that Li ion conductivity could be enhanced in the vicinity of nano-sized ceramic particles.

Several studies have been conducted on the electrochemical properties of non-graphitizable carbon electrodes [9–11]. Non-graphitizable carbon has different electrochemical properties, depending on the nature of the precursor. Dahn et al. [9] studied the electrochemical behavior of some types of non-graphitizable carbon in a liquid electrolyte, and reported that non-graphitizable carbon had a higher reversible capacity than graphitic carbon ($\sim$372 mAh g^{-1}). Composites consisting of non-graphitizable carbon and other active materials, for example tin and silicon, have also been studied to improve the energy density of Li-ion batteries [12–14]. For instance, Wilson and Dahn [12] prepared Si–non-graphitizable carbon composite electrodes by chemical vapor deposition, and reported additional reversible capacity because of nano-sized particles of Si. However, little attention has been paid to composites consisting of non-graphitizable carbon and inactive materials such as SiO_2.

In this work, we prepared SiO_2–non-graphitizable carbon composite electrodes as a model electrode consisting of a battery active material and electrochemically inactive nano-materials. As noted above, the lithium ion transport properties should be enhanced by addition of nano-materials in the composite electrodes, resulting in an increase in the utilization of the active materials. The effects of SiO_2 on Li ion transfer at the electrode–electrolyte interface, as measured by ac impedance spectroscopy, are also discussed.

2 Experimental

2.1 Preparation and characterization of SiO_2–non-graphitizable carbon composites

Carbonaceous materials were prepared as follows. Ethyl cellulose (Nacalai Tesque) was dissolved in ethanol (Nacalai Tesque) at an ethyl cellulose-to-ethanol ratio of 5:95. The solution was heated at 473 K in air for 12 h and then cooled to room temperature. The products were further heated to 1,273 K at 10 K min^{-1} under an air atmosphere and held at this temperature for 1 h. The rate of the weight decrease was evaluated from the ratio of the resulting carbonaceous materials to ethyl cellulose. This value was used to determine the ratio of SiO_2 to non-graphitizable carbon for SiO_2–non-graphitizable carbon composites. SiO_2–non-graphitizable carbon composites were prepared by a method similar to that of carbonaceous materials, except that we added SiO_2 particles (Nanophase Technologies, NanoTeck SiO_2, average particle size 25 nm) to an ethyl cellulose–ethanol solution at different ratios. The resulting materials were characterized by X-ray diffraction (XRD, RINT2500, Rigaku) and Raman spectroscopy (T-64000, Jobin Yvon). Their morphology were investigated by scanning electron microscopy (SEM).

2.2 Electrochemical measurements

Electrochemical properties were studied by charge–discharge measurements at a constant current rate of 62 mA (carbon g)$^{-1}$ using a three-electrode cell. The working electrode was prepared by coating copper foil with a mixture of the resulting materials (90 wt%) and poly(vinylidene fluoride) (10 wt%) dissolved in 1-methyl-2-pyrrolidone.

The electrode was then dried in a vacuum for 8 h at 393 K. A liquid electrolyte of 1 mol dm^{-3} $LiClO_4$ dissolved in EC + DEC (1:1 by volume) was used. Lithium metal was used for both the counter and reference electrodes. Unless otherwise stated, the potential is given versus Li/Li^+.

Li ion transfer at the interface between the electrode and electrolyte was investigated by ac impedance spectroscopy using a VoltaLab80 (Radiometer Analytical SAS). After each cycle of charge and discharge measurements, the

electrode was swept to a given potential (from 0.6 to 3.0 V) at 1.0 mV s^{-1} and kept at that potential to reach a steady state. Ac impedance spectra were then obtained by applying a sine wave with an amplitude of 10 mV over a frequency range from 100 kHz to 10 mHz.

All experiments were conducted under an argon atmosphere with a dew point below −60°C.

3 Results and discussion

3.1 Characterization

Figure 1 shows XRD patterns for (a) the resulting composite prepared by pyrolyzing a mixture of SiO_2 and ethyl cellulose, (b) SiO_2 particles, and (c) carbonaceous materials obtained from ethyl cellulose. In Fig. 1a, very broad peaks were observed at $2\theta \approx 22°$ and 44°. The peak at approximately 44° was assigned to the carbonaceous materials in the composite, because carbonaceous materials obtained from ethyl cellulose gave a peak at approximately 44°, as shown in Fig. 1c. On the other hand, SiO_2 and carbonaceous materials had diffraction peaks at 22 and 26°, respectively, as shown in Fig. 1b, c. These two peaks gave a very broad peak in Fig. 1a. These results indicate that a composite of SiO_2 and carbonaceous materials was obtained by pyrolyzing a mixture of SiO_2 and ethyl cellulose.

Figure 2 shows Raman spectra of the composite and carbonaceous materials that had been prepared from ethyl cellulose. Two main peaks appeared at approximately 1,360 and 1,600 cm^{-1}. The peak at approximately 1,580 cm^{-1} is well known to be related to the crystallinity of carbonaceous materials, and is assigned to the Raman-active E_{2g} mode frequency (G band) [15]. The peak at approximately

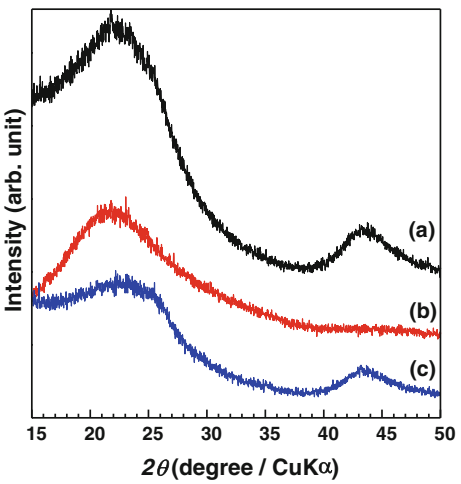

Fig. 1 X-ray diffraction patterns of (*a*) a SiO_2 (2.75 wt%)–carbon composite, (*b*) SiO_2, and (*c*) carbonaceous material prepared from ethyl cellulose

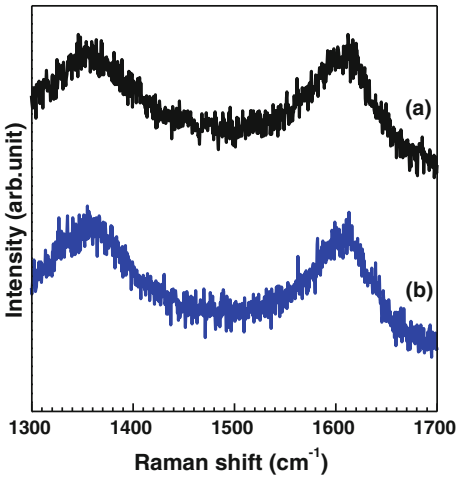

Fig. 2 Raman spectra of (*a*) a SiO_2 (2.75 wt%)–carbon composite and (*b*) carbonaceous material prepared from ethyl cellulose

1,360 cm^{-1} is ascribed to the Raman-inactive A_{1g} mode frequency [15]. The peaks at approximately 1,360 and 1,620 cm^{-1} appear when crystal size is finite and there are imperfections in the carbonaceous materials; the former is called a D band and the latter is a D′ band. The shape of the spectra in Fig. 2 is similar to that of typical low-crystalline carbon. In addition, no obvious difference was observed between the spectra, suggesting that the crystallinity of non-graphitizable carbon was not affected by pyrolysis with SiO_2.

Figure 3 shows SEM images of (a) the SiO_2 (3 wt%)–non-graphitizable carbon composite, (b) the SiO_2 (20 wt%)–non-graphitizable carbon composite, and (c) non-graphitizable carbon. Particles smaller than 100 nm (white color) were observed on the surface of non-graphitizable carbon fragments in Fig. 3a, b, whereas such particles were not seen in Fig. 3c. The number of small particles increased with increasing SiO_2 content, and, therefore, these particles were identified as SiO_2.

3.2 Electrochemical properties

Figure 4 shows the charge and discharge curves of an SiO_2 (20 wt%)–non-graphitizable carbon composite and non-graphitizable carbon prepared from ethyl cellulose. In the 1st cycle, a large irreversible capacity, which is defined as a capacity that is not recovered in the subsequent discharge process, was observed, and was evaluated to be 360 and 234 mAh (carbon g)$^{-1}$ for the composite electrode and the non-graphitizable carbon electrode, respectively. The composite electrode gave larger irreversible capacity than the non-graphitizable carbon electrode in the 1st cycle. If the irreversible reactions between SiO_2 and Li ions are responsible for the large irreversible capacity, the internal resistance of the composite electrode should be large, because of the insulating products of Li_2O. However, this is not the case,

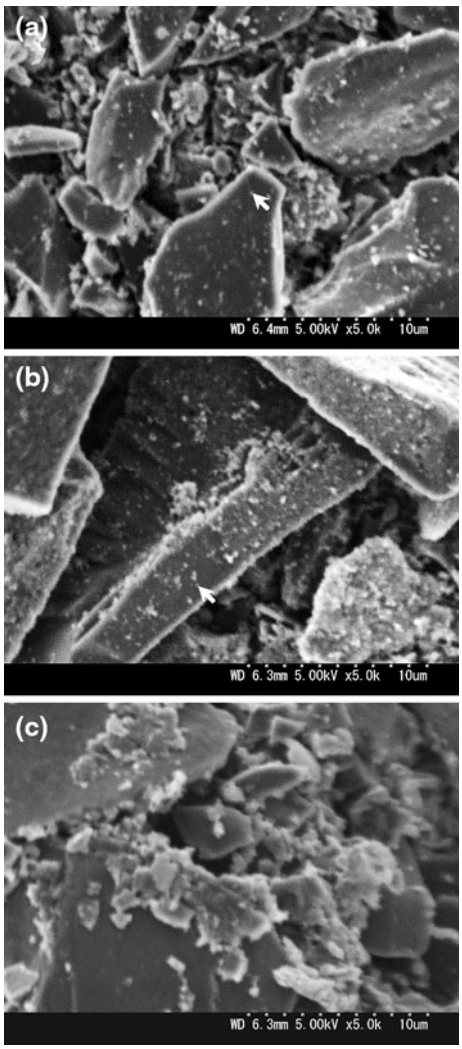

Fig. 3 SEM images of **a** a SiO_2 (3 wt%)–non-graphitizable carbon composite, **b** a SiO_2 (20 wt%)–non-graphitizable carbon composite, and **c** non-graphitizable carbon prepared from ethyl cellulose. For clarity, SiO_2 particles are indicated by *arrows* in **a** and **b**

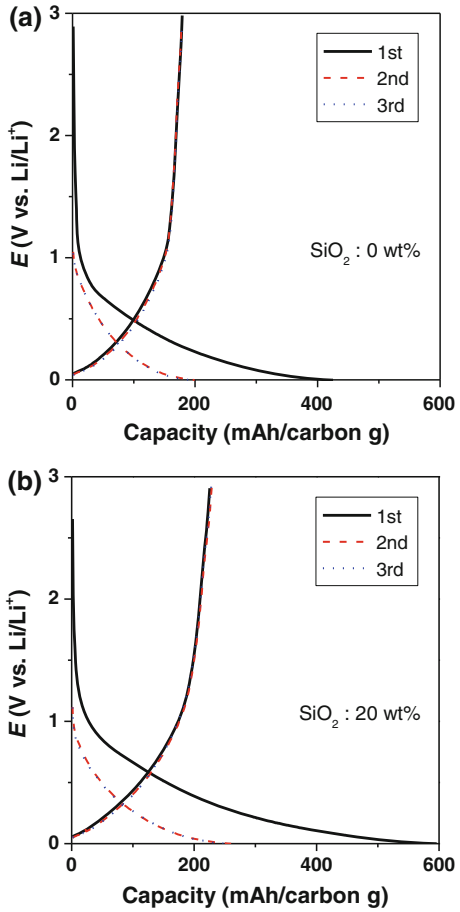

Fig. 4 Charge and discharge curves for **a** a non-graphitizable carbon electrode and **b** an SiO_2 (20 wt%)–non-graphitizable carbon composite electrode in 1 mol dm^{-3} $LiClO_4$ dissolved in EC + DEC (1:1 by volume)

as shown later in Fig. 7. The irreversible capacity can be attributed to irreversible reactions during the insertion and reactions of Li ion at non-graphitizable carbon, as is often reported in the literature [9]. After the 2nd cycle, the irreversible capacity dramatically decreased and obvious symmetry was seen in the charge–discharge curves; a uniform decrease and increase in potential was observed below 1.0 V during the charge and discharge reactions, respectively. The reversible capacity for the composite electrode (225 mAh (carbon g)$^{-1}$) was larger than that for the non-graphitizable carbon electrode (178 mAh (carbon g)$^{-1}$). Although the detailed mechanism of the increase in capacity for composite electrodes is not yet clear, the utilization ratio of non-graphitizable carbon in terms of Li ion insertion seemed to be improved by SiO_2, and, hence, both the reversible and irreversible capacities increased. Note that the reversible capacity of non-graphitizable carbon electrodes could be increased by addition of SiO_2, whereas SiO_2 can hardly accommodate any Li ion.

Figure 5 shows the relationship between the discharge capacity of SiO_2–non-graphitizable carbon composite electrodes during the 1st, 2nd, and 3rd cycles and the SiO_2 content in the composites. The reversible capacity gradually increased with an increasing SiO_2 content above 5 wt%, whereas similar values of approximately 180 mAh (carbon g)$^{-1}$ were obtained below 3 wt%.

Figure 6 shows Nyquist plots of the composite electrode at potentials of 0.6, 0.8, and 0.9 V using 1 mol dm^{-3} $LiClO_4$ dissolved in EC + DEC (1:1 vol.). Each measurement was conducted at ca. 25 °C after charge and discharge measurements. One semi-circle was observed in the high-frequency region (>100 Hz) at potentials above 1.0 V. On the basis of the charge and discharge curves, no insertion and extraction of Li ion occurred at potentials above 1.0 V. In addition, this semi-circle was not affected by the electrode potential even at potentials below 1.0 V, as shown in the

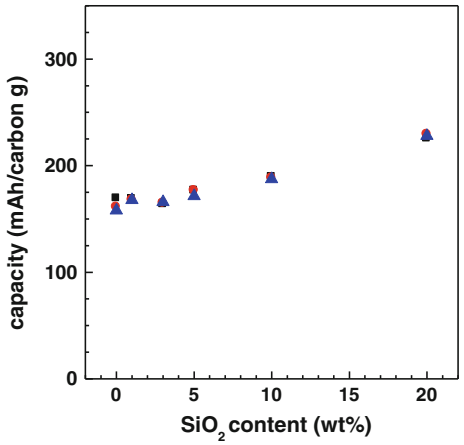

Fig. 5 Discharge capacities of SiO_2–non-graphitizable carbon composite electrodes in the 1st (*squares*), 2nd (*circles*), and 3rd (*triangles*) cycles as a function of SiO_2 content

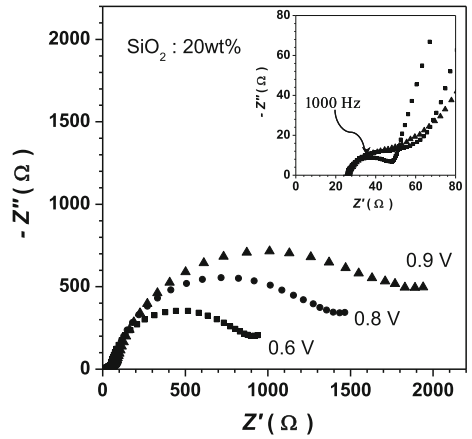

Fig. 6 Impedance spectra of an SiO_2 (20 wt%)–non-graphitizable carbon composite electrode in 1 mol dm^{-3} $LiClO_4$ dissolved in EC + DEC (1:1 by volume) at potentials of 0.6 (*squares*), 0.8 (*circles*), and 0.9 V (*triangles*)

inset in Fig. 6. Therefore, this resistance is because of the surface film that was formed on the composite electrode. At potentials below 0.9 V, another semi-circle appeared in the mid to low-frequency region (<100 Hz). The dimension of the semi-circle in the low-frequency region depended on the electrode potential: the values of the resistance, which can be evaluated from the real part of the impedance of the semi-circle, decreased with decreasing electrode potential. The semi-circles could not be ascribed to electronic resistance of the composite electrodes, because non-graphitizable carbon has a very large electronic conductivity. Hence, the resistance should be identified as the charge-transfer resistance (R_{ct}) because of Li ion transfer at the interface between the composite electrode and electrolyte. The value of R_{ct} was evaluated by fitting the semi-circle in the low-frequency region by using a parallel equivalent circuit of the constant

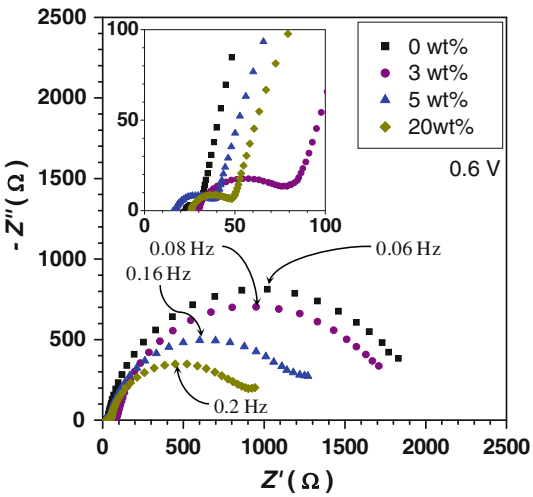

Fig. 7 Impedance spectra of SiO_2–non-graphitizable carbon composite electrodes containing 0 wt% (*squares*), 3 wt% (*circles*), 5 wt% (*triangles*), and 20 wt% (*diamonds*) SiO_2

phase element and R_{ct} [16]. Almost identical Nyquist plots were obtained for composites with different proportions of SiO_2. Figure 7 shows that impedance spectra of SiO_2–non-graphitizable carbon composite electrodes at 0.6 V. R_{ct} decreased with increasing SiO_2 content in the composites, particularly above 5 wt%; the values of R_{ct} were in the order $0 > 3 > 5 > 20$ wt%. If non-graphitizable carbon is oxidized by SiO_2 at elevated temperatures during calcination, the surface structure of non-graphitizable carbon should change and the number of Li ion insertion sites on it would increase, which would lead to a decrease in R_{ct} [4, 17]. However, Ellingham diagrams indicate that carbonaceous materials are not oxidized by SiO_2 at a calcination temperature of 1,273 K. Hence, the decrease in R_{ct} of the composites is not because of an increase in Li ion insertion sites on the non-graphitizable carbon. As shown in the inset in Fig. 7, the values of the surface film resistance were in the order $3 > 5 > 20 > 0$ wt%. Hence, the surface film resistance seems to be independent of the SiO_2 content of the composites. The electronic and electrolyte resistance, which is identified as the resistance at the intersection of the higher-frequency end of the surface film resistance on the real axis, was also not associated with the SiO_2 content of the composites; the values of the electrolyte resistance were in the order $3 > 20 > 0 > 5$ wt%. These resistance values would be affected by the thickness and the porosity of the composite electrodes [6]. In this study the composite containing 3 wt% SiO_2 had the largest resistance, because of the electrolyte and surface films; this is likely to be because of the thick composite electrode. SiO_2 is an electron insulator, and, hence, the electronic resistance should increase with increasing SiO_2 content of the composites. In fact, the composite containing 20 wt% SiO_2 had a larger value

(ca. 25 Ω) at the initial rise of the semi-circle, because of the surface films, than those containing 0 and 5 wt% SiO_2. On the other hand, R_{ct} consistently decreased with increasing SiO_2 content of the composites. These results indicate that these composite electrodes can serve as model electrodes to examine the phase-transfer kinetics of the Li ion between electrode and electrolyte. On the basis of the results that the reversible capacity increased and R_{ct} decreased with increasing SiO_2 content, the insertion and extraction reactions of Li ions at composite electrodes are controlled by Li ion transfer at the electrode–electrolyte interface. Thus, SiO_2 nano-sized particles on non-graphitizable carbon facilitated Li ion transfer at the interface between a non-graphitizable carbon electrode and an electrolyte, and the utilization ratio of non-graphitizable carbon in terms of Li ion storage was improved by the decrease in R_{ct}. On the basis of these results, a decrease in R_{ct} and an increase in the reversible capacity can both be obtained by formation of SiO_2–non-graphitizable carbon composites; this would lead to Li-ion batteries with high power and energy density.

4 Conclusion

SiO_2–non-graphitizable carbon composites were prepared by pyrolyzing a mixture of ethyl cellulose and nano-sized SiO_2 particles. For the composite electrodes, high reversibility of insertion and extraction reactions of the Li ion was observed after the 2nd cycle, whereas large irreversible capacity was observed in the 1st cycle. The reversible capacity increased with increasing SiO_2 content above 5 wt%, whereas SiO_2 can hardly accommodate any Li ion. R_{ct} because of Li ion transfer at the electrode–electrolyte interface decreased with increasing SiO_2 content above 5 wt%. These results suggest that SiO_2 nano-sized particles on non-graphitizable carbon facilitated Li ion transfer at the interface between a non-graphitizable carbon electrode and an electrolyte, which improved the utilization ratio of non-graphitizable carbon in terms of Li ion storage.

Acknowledgments This work was supported by an Industrial Technology Research Grant in 2000 from the New Energy and Industrial Technology Development (NEDO) of Japan and also by a Grant-in-Aid for the 21st century program—COE for a United Approach to New Materials Science—from the Ministry of Education, Culture, Sports, Science, and Technology.

References

1. Winter M, Besenhard JO, Spahr ME, Novak P (1998) Adv Mater 10:725
2. Ogumi Z, Inaba M (1998) Bull Chem Soc Jpn 71:521
3. Doi T, Miyatake K, Iriyama Y, Abe T, Ogumi Z, Nishizawa T (2004) Carbon 42:3183
4. Doi T, Iriyama Y, Abe T, Ogumi Z (2005) J Electrochem Soc 152:A1521
5. Iriyama Y, Kurita H, Yamada I, Abe T, Ogumi Z (2004) J Power Sources 137:111
6. Sawai K, Ohzuku T (2003) J Electrochem Soc 150:A674
7. Mizuhata M, Kitamura M, Kajinami A, Deki S (2003) In: Abstract of 70th Electrochemical Society of Japan, 1M31
8. Croce F, Curini R, Martinelli A, Persi L, Ronci F, Scrosati B (1999) J Phys Chem B 103:10632
9. Dahn JR, Zheng T, Liu YH, Xue JS (1995) Science 270:590
10. Iijima T, Suzuki K, Matsuda Y (1995) Synth Met 73:9
11. Sato K, Noguchi M, Demachi A, Oki N, Endo M (1994) Science 264:56
12. Wilson AM, Dahn JR (1995) J Electrochem Soc 142:326
13. Tamai H, Matsuoka S, Ishihara M, Yasuda H (2001) Carbon 39:1515
14. Liu Y, Hanai K, Yang J, Imanishi N, Hirano A, Takeda Y (2004) Solid State Ion 168:61
15. Tuinstra F, Koenig JL (1970) J Chem Phys 53:1126
16. Funabiki A, Inaba M, Abe T, Ogumi Z (1999) J Electrochem Soc 146:2443
17. Xue JS, Dahn JR (1995) J Electrochem Soc 142:3668